ISSN 0036-0244, Russian Journal of Physical Chemistry A, 2020, Vol. 94, No. 4, pp. 806–809. © Pleiades Publishing, Ltd., 2020.
Russian Text © The Author(s), 2020, published in Zhurnal Fizicheskoi Khimii, 2020, Vol. 94, No. 4, pp. 585–589.

PHYSICAL CHEMISTRY OF NANOCLUSTERS AND NANOMATERIALS

Effect of the Morphology of γ-Al_2O_3 Nanosized Particles on Their Adsorption Properties

S. O. Kazantsev[a], E. A. Glazkova[a], A. S. Lozhkomoev[a], O. V. Bakina[a,*], and E. G. Khorobraya[a]

[a] *Institute of Strength Physics and Materials Science, Siberian Branch, Russian Academy of Sciences, Tomsk, 634055 Russia*

**e-mail: ovbakina@ispms.tsc.ru*

Received May 13, 2019; revised May 13, 2019; accepted June 18, 2019

Abstract—γ-Al_2O_3 porous nanostructures with different morphologies are prepared from an aluminitride nanopowder (obtained by electric explosion) by treatment with water under various conditions. Depending on the parameters of oxidation, the morphology of the nanostructures includes nanosheets, nanoplates, and nanorods. The structures are characterized via transmission electron microscopy, X-ray diffraction, and thermal nitrogen adsorption–desorption. The adsorption of reference cationic and anionic dyes from aqueous solutions is used as an example to analyze the sorption properties of the nanostructures. It is shown that the Sips model is the one closest to the experimental adsorption isotherm for all γ-Al_2O_3 samples, regardless of their morphology. It is found that nanorods have the highest adsorption capacity with respect to eosin, while methylene blue is adsorbed similarly by nanorods and nanoplates. It is concluded that the obtained nanostructures can be used as promising materials for water purification, due to the simplicity of their synthesis and their high adsorption characteristics.

Keywords: nanostructures, water purification, adsorption

DOI: 10.1134/S0036024420030139

INTRODUCTION

The synthesis of nanostructured adsorbents having different morphology and surface properties for wastewater treatment is currently of great interest. Techniques that allow us to vary the properties of nanoparticles during synthesis make it possible to obtain materials with new unique properties. Aluminum oxide nanostructures are important inorganic materials widely used in water treatment technologies, due to their high efficiency of adsorption [1]; thermal [2], chemical, and mechanical [3] stability; and low toxicity [4]. The γ-Al_2O_3 phase is the best of the different crystalline aluminum ones, due to its thermodynamic stability and special microstructural properties [5]. A number of γ-Al_2O_3 nanostructures with different morphologies have already been obtained: nanotubes for efficiently removing dyes [6]; nanofibers for removing fluoride ions [7]; three-dimensional microspheres [8] and nanospheres for removing cations [9]; and nanocrystals [10] and nanoflakes [11]. The ways of preparing these, however, often have its limitations because of their complex procedures of synthesis, high cost, and the toxicity of the initial materials. Aluminum and aluminum nitride nanopowders obtained via the electric exploding of conductors as precursors allow us to obtain γ-Al_2O_3 nanostructures with large specific surfaces and positive surface charges. This technique is simple and environmentally friendly; the reaction of aluminum oxidation proceeds at a low temperature (60°C); and the only initial reagents are aluminum nanopowder and water, which contributes to the formation of chemically pure products, the calcination of which produces γ-Al_2O_3 of different morphologies.

EXPERIMENTAL

The procedure in [12] requiring the oxidation of Al/AlN nanoparticles with water under various conditions was used to obtain γ-Al_2O_3 with different morphologies. Boehmite nanosheets were prepared via oxidation of AlN/Al nanoparticles with water at 60°C. Boehmite nanoplates were obtained via the water oxidation of AlN/Al nanoparticles under hydrothermal conditions at elevated pressure and 200°C over 6 h. Hexagonal rods were prepared via the oxidation of AlN/Al nanoparticles in moist air at 60°C and a relative humidity of 80%. γ-Al_2O_3 nanostructures were obtained via the thermal treatment of boehmite nanoparticles at 500°C over 2 h.

The resulting samples were studied via transmission electron microscopy (JEM-2100, Japan), X-ray diffraction (Shimadzu XRD 7000, Japan), IR spectroscopy (Nicolet 5700, Thermo Electron, United States), and thermal nitrogen desorption (Sorbtometr M, Russia). The specific surfaces of the samples were calculated using the BET model.

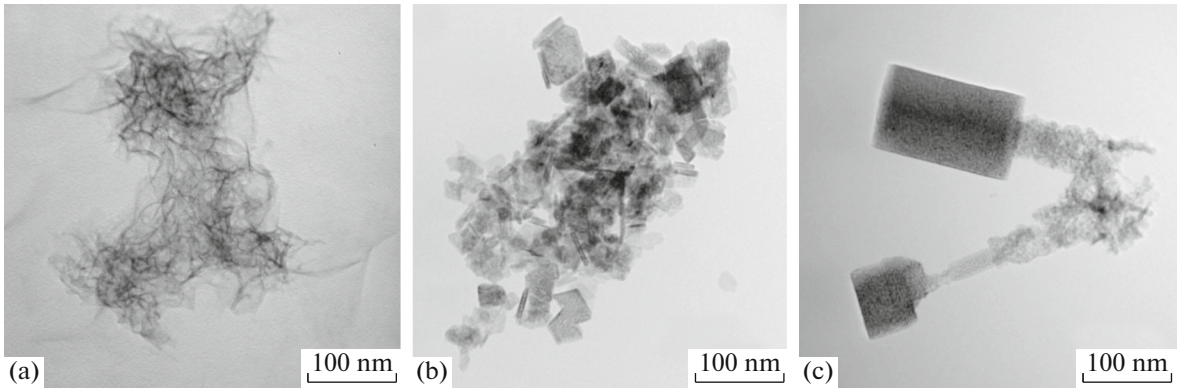

Fig. 1. Electron microscopic images of γ-Al_2O_3 nanostructures: (a) nanosheets, (b) nanoplates, and (c) nanorods.

Reference adsorbates (anionic eosin and cationic methylene blue dyes) were used for adsorption experiments; 5 mL of a dye solution was added to 0.1 g of nanostructures to study their kinetics and to construct an adsorption isotherm. Samples were taken at certain time intervals, centrifuged at 3500 rpm, and analyzed on a SF spectrophotometer at a wavelength of 490 nm for eosin and 660 nm for methylene blue. The optical path of the cuvette was 10 mm.

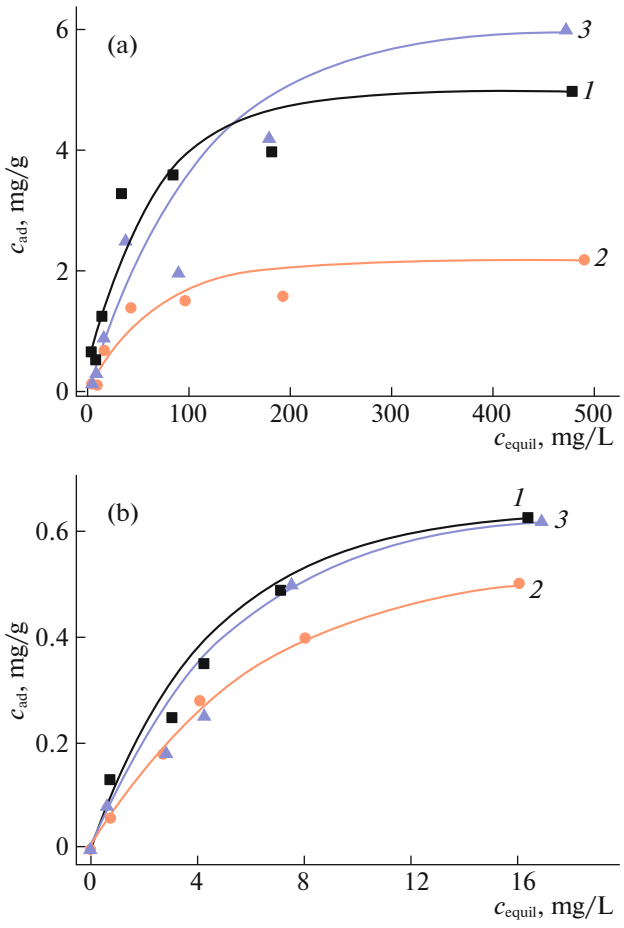

Fig. 2. (Color online) Adsorption isotherms of: (a) eosin and (b) methylene blue on the surface of: (*1*) nanosheets, (*2*) nanoplates, and (*3*) hexagonal rods agolmerates.

To describe the kinetics of adsorption, we employed (1) the Langmuir model, in which adsorption is limited by the formation of a sorbate monolayer, the surface of a sorbent is uniform, the energy of sorption is constant for all sorption centers, and there is no interaction between the sorbate molecules; (2) the Freundlich model of empirical sorption, characterized by the probability of multilayer adsorption; (3) the Sips model, which combines the Langmuir and Freundlich models, indicates the limiting sorption value upon an increase in the concentration of the sorbate, and describes sorption on a heterogeneous surface without the interaction between sorbate molecules; and (4) the Dubinin–Radushkevich model, which is used to assess the characteristic porosity and the apparent adsorption activation energy.

RESULTS AND DISCUSSION

Figure 1 shows electron microscope images of γ-Al_2O_3 nanostructures. It is clear that the γ-Al_2O_3 nanostructures obtained from products of the water oxidation of AlN/Al nanoparticles at 60°C were agglomerates of folded nanosheets around 2–5 nm thick with planar sizes of 100–200 nm (Fig. 1a). The γ-Al_2O_3 sample obtained from the products of hydrothermal oxidation was a nanoplate 20–100 nm in size and 5–30 nm thick (Fig. 1b). The samples obtained via calcination of the products of the oxidation of AlN/Al nanopowder in moist air were rods 50–400 nm long and 50–150 nm in diameter with a hexagonal cross section (Fig. 1c).

The X-ray diffraction patterns of the synthesized samples contain the same set of reflections at 22.6, 37.3, 43.9, 46.2, 53.8, 72.1, and 79.8 that are characteristic of planes (111), (220), (311), (222), (400), (511), and (440). These diffraction peaks are in good agree-

Table 1. Model parameters of eosin sorption on γ-Al_2O_3 samples with different morphologies

Model	q_{max}, mg/g	K	Exponent	R^2
Nanosheet agglomerates				
Langmuir	5.059	0.3009	—	0.8750
Freundlich	—	0.6906	0.331	0.9432
Sips	4.985	0.0284	1.0377	0.896
Dubinin–Radushkevich	4.146	3.857×10^{-5}	—	
Nanoplates				
Langmuir	2.222	0.0165	—	0.831
Freundlich	—	0.1778	0.408	0.837
Sips	4.429	0.0283	0.568	0.737
Dubinin–Radushkevich	1.572	—	—	
Hexagonal rods				
Langmuir	7.920	0.0062	—	0.943
Freundlich	—	0.242	0.874	0.95
Sips	11.92	0.0107	0.740	0.766
Dubinin–Radushkevich	6.05	0.0015	—	0.766

ment with the cubic structure of γ-Al_2O_3 (JCPDS 00-010-0425). All of the nanostructures synthesized after heat treatment at 500°C therefore had the same phase composition.

The IR spectra of the samples have the same sets of absorption bands: high-intensity bands caused by valence vibrations of Al–O group; bands at 1395 cm^{-1} corresponding to the characteristic vibrational structure of the γ-Al_2O_3 lattice [13]; and low-intensity bands at 1644 cm^{-1}, attributed to the vibrations of adsorbed water [14]. The broadened bands at 3800–3000 cm^{-1} correspond to hydrogen bonds between the different hydroxyl groups in the samples [15].

The nitrogen adsorption–desorption isotherms have the typical S-shape. The isotherms for nanosheets and nanoplates are of type IV (IUPAC), so the samples were of a predominantly mesoporous structure. The adsorption of nitrogen resulted in capillary-condensation hysteresis (p/p_0) from 0.5 to 0.9, and the narrower loop is characteristic of nanoplates. The maximum pore size distribution corresponds to 10 nm, and the specific surface areas are 267 m^2/g for nanoplates and 106 m^2/g for nanosheets.

The adsorption–desorption isotherm obtained for hexagonal rods is of type V, which is characteristic of weak gas–solid interaction on mesoporous and microporous adsorbents. The hexagonal rods had a specific surface area of 249 m^2/g and microporosity with the maximum pore distribution only in the range of less than 2 nm.

Figure 2 shows the adsorption isotherms of eosin and methylene blue, obtained for γ-Al_2O_3 nanostructures of various morphologies.

Eosin is an anionic dye that is adsorbed on surfaces of γ-Al_2O_3 mainly because of electrostatic interaction. When the specific surface area of the samples was increased, the adsorption of dye grew as well, and maximum adsorption was achieved on γ-Al_2O_3 rods (Fig. 2a, curve *3*). Methylene blue is a cationic dye that is weakly adsorbed on surfaces of γ-Al_2O_3 regardless of the morphology and pore size of the samples (Fig. 2b).

Tables 1 and 2 show the values of the parameter of the adsorption isotherm models and coefficients R^2 of reliability.

With γ-Al_2O_3 nanoplates, the R^2 values show that the adsorption of dyes is best described by the Sips equation (Tables 1 and 2). The q_{max} values indicate that the main centers predominate on the surfaces of γ-Al_2O_3 nanoplates. The surface of the sorbent is energetically uniform, and the multilayer adsorption of eosin proceeds. At the same time, the adsorption of methylene blue is rather weak.

The adsorption of the base and acid dyes on hexagonal γ-Al_2O_3 rods is described by the Sips and Freundlich models (Tables 1 and 2). The multilayer adsorption of eosin is preferred, and the surface is energetically quite uniform. A strongly energetic inhomogeneous surface appears upon the sorption of methylene blue, so adsorption is rather weak. The R^2 values show that the adsorption of dyes on γ-Al_2O_3 nanosheets is best described with the Sips equation (Tables 1 and 2). The q_{max} values indicate that the main centers predominate in the agglomerates of nanosheets. The Sips and Langmuir models are close for the adsorption of eosin, so we may conclude that the surface of the sorbent is in this case energetically homogeneous; in addition, monolayer adsorption is

Table 2. Model parameters of the sorption of methylene blue on γ-Al_2O_3 samples of different morphology

Model	q_{max}, mg/g	K	Exponent	R^2
Nanosheet agglomerates				
Langmuir	0.869	0.1621	—	0.9889
Freundlich	—	0.1703	0.478	0.9839
Sips	5.576	0.0306	0.519	0.9852
Dubinin–Radushkevich	0.848	4.924×10^{-6}	—	0.969
Nanoplates				
Langmuir	0.739	0.1370	—	0.9959
Freundlich	—	0.1176	0.539	0.9795
Sips	0.623	0.1313	1.246	0.9976
Dubinin–Radushkevich	0.892	7.23×10^{-6}	—	0.952
Hexagonal rods				
Langmuir	1.061	0.0898	—	0.9737
Freundlich	—	0.1195	0.599	0.9608
Sips	0.710	0.0516	1.785	0.9796
Dubinin–Radushkevich	0.715	4.88×10^{-6}	—	0.959

observed. The sorption of methylene blue is weak, and the surface of the sorbent is energetically heterogeneous.

These models are usually empirical or idealized, so several of them allow more complete description of the parameters of a sorbent. The models' high values of coefficient R^2 indicate they are adequate and the considered parameters are reliable.

CONCLUSIONS

Our analysis of the sorption properties of γ-Al_2O_3 nanostructures during the adsorption of reference eosin and methylene blue dyes from aqueous solutions showed that the Sips model is closest to the experimental adsorption isotherm. This indicates that the surface of the adsorbents is energetically heterogeneous and that there is multilayer adsorption. Rod nanostructures display the maximum degree of adsorption.

FUNDING

This work was performed as part of the Program of Fundamental Scientific Studies of the State Academies of Sciences for 2013–2020 (direction III.23).

REFERENCES

1. V. Tomar and D. Kumar, Chem. Centr. J. **7** (2013). https://doi.org/10.1186/1752-153X-7-5
2. L. H. Song and S. B. Park, J. Nanosci. Nanotechnol. **10**, 122 (2010).
3. M. Ozawa and Y. Nishio, Appl. Surf. Sci. **380**, 288 (2016).
4. D. Krewski, R. A. Yokel, E. Nieboer, D. Borchelt, et al., J. Toxicol. Environ. Health **10**, 1 (2007).
5. S. Zhou, M. Antonietti, and M. Niederberger, Small **3**, 763 (2007).
6. Z. Shu, Y. Chen, J. Zhou, T. Li, et al., Appl. Clay Sci. **112**, 17 (2015).
7. A. Mahapatra, B. G. Mishra, and G. Hota, Ind. Eng. Chem. Res. **52**, 1554 (2013).
8. X. Song, P. Yang, C. Jia, et al., RSC Adv. **5**, 33155 (2015).
9. T. P. M. Chu, N. T. Nguyen, T. L. Vu, et al., Materials **12**, 450 (2019).
10. Y. Zhang, Y. Ye, Z. Liu, et al., J. Alloys Compd. **662**, 421 (2016).
11. E. Yu, H. J. Lee, T. Ko, et al., Nanoscale **5**, 10014 (2013).
12. S. O. Kazantsev, A. S. Lozhkomoev, E. A. Glazkova, et al., Mater. Res. Bull. **104**, 97 (2018).
13. C. Zhang, Z. Liu, L. Chen, and Y. Dong, J. Radioanal. Nucl. Chem. **292**, 411 (2012).
14. J. Gangwar, B. K. Gupta, S. K. Tripathi, and A. Srivastava, Nanoscale **7**, 13313 (2015).
15. S. A. Hosseini, A. Niaei, and D. Salari, Open J. Phys. Chem. **1** (02), 23 (2015).

Translated by A. Tulyabaev